

# Inheritance Between Feedforward and Convolutional Networks via Model Projection

Nicolas Ewen<sup>1</sup> Jairo Diaz-Rodriguez<sup>1</sup> Kelly Ramsay<sup>1</sup>

## Abstract

Techniques for feedforward networks (FFNs) and convolutional networks (CNNs) are frequently reused across families, but the relationship between the underlying model classes is rarely made explicit. We introduce a unified node-level formalization with tensor-valued activations and show that generalized feedforward networks form a strict subset of generalized convolutional networks. Motivated by the mismatch in per-input parameterization between the two families, we propose model projection, a parameter-efficient transfer learning method for CNNs that freezes pretrained per-input-channel filters and learns a single scalar gate for each (output channel, input channel) contribution. Projection keeps all convolutional layers adaptable to downstream tasks while substantially reducing the number of trained parameters in convolutional layers. We prove that projected nodes take the generalized FFN form, enabling projected CNNs to inherit feedforward techniques that do not rely on homogeneous layer inputs. Experiments across multiple ImageNet-pretrained backbones and several downstream image classification datasets show that model projection is a strong transfer learning baseline under simple training recipes.

## 1. Introduction

Modern transfer learning with convolutional neural networks (CNNs) often faces a practical tension. Full fine-tuning adapts all layers to a downstream task, but can overfit when labeled data are scarce and can be expensive in parameters and optimization effort (Chollet, 2021). Partial fine-tuning reduces overfitting risk by training only a subset of parameters (often the final layers), but this can limit how much the pretrained representation can adapt to do-

<sup>1</sup>Department of Mathematics and Statistics, York University, Toronto, Ontario M3J 1P3, Canada. Correspondence to: Nicolas Ewen <gnic@my.yorku.ca>.

Preprint. February 9, 2026.

main shift (Kornblith et al., 2019). We propose a simple alternative that keeps the entire network trainable in a structured way while drastically reducing the number of trainable parameters inside convolutional layers.

**Model projection.** Consider a convolutional node that maps  $d$  input channels to an output channel using a learned filter per input channel. Instead of fine-tuning all filter weights, we *freeze* the pretrained filters and introduce a new trainable scalar  $\gamma_{jk}$  for each (output channel  $j$ , input channel  $k$ ), which scales that input channel's contribution to the output. Biases remain trainable. Intuitively, projection turns each convolutional node into: (i) a fixed, pretrained per-channel feature extractor (the frozen filter), followed by (ii) a learned channel-wise linear recombination (the  $\gamma$  weights) before the nonlinearity. This reduces the number of trainable parameters in a typical  $k_1 \times k_2$  convolution from on the order of  $d_{\text{out}}d_{\text{in}}k_1k_2$  to on the order of  $d_{\text{out}}d_{\text{in}}$  (plus biases), while still allowing *every* convolutional node to adapt to the downstream task (See Fig. 1).

In our experiments, projection serves as an effective transfer learning method across multiple ImageNet-pretrained backbones and several datasets, often yielding strong performance under simple training recipes. Projection is designed to recover a specific and widely used property of traditional feedforward neural networks (FFNs), namely training a node with one scalar weight per input channel, in settings where CNN nodes ordinarily contain many weights per input channel. This example motivates a more general question: *when is it legitimate to transfer results and techniques between model classes?*

**Inheritance between model classes.** We study this question of *inheritance*: when can results, techniques, and guarantees developed for one model class be automatically applied to another? FFNs and CNNs are a natural test case. They are both compositions of simple node computations, yet they are typically formalized differently and studied by partly different communities (Hastie et al., 2009; LeCun et al., 2010; Goodfellow et al., 2016). This mismatch makes it difficult to state precise relationships between the corresponding model classes, and therefore difficult to make clear inheritance claims.

**A unified formalization.** To consider inheritance rigorously, we introduce a general node-level formalization that handles tensor-valued inputs. We define a generalized FFN (GFFN) node that performs a weighted sum across input channels while preserving the per-channel tensor structure, and a generalized CNN (GCNN) node that performs channel-wise convolutions and then sums across channels. Under this framework, we show that GFFNs are a strict subset, or subclass, of GCNNs. Informally, a convolution with kernel size one in every spatial dimension reduces to channel-wise weighted summation, matching the GFFN node computation. This set inclusion immediately yields one direction of inheritance: any result that holds for all GCNNs also holds for all GFFNs.

**Recovering inheritance via projection.** In the opposite direction, we show that CNNs cannot always inherit FFN techniques. However, our proposed model projection allows for inheritance from FFNs to CNNs by exploiting a structural property of CNN node functions: separability by input channel before the nonlinearity. Freezing the per-channel transformations and introducing one trainable scalar per channel contribution yields projected nodes that match the GFFN form up to allowing inhomogeneous inputs across nodes. As a result, projected CNNs can inherit FFN results and techniques that do not rely on homogeneous inputs.

**Evaluating model projection.** We analyze the training behavior and robustness of model projection across multiple benchmarks using ImageNet-pretrained backbones. These experiments show that model projection combines the rapid initial improvement characteristic of partial tuning with the continued performance gains of end-to-end optimization, while exhibiting improved stability on smaller datasets. Second, we compare model projection to established parameter-efficient transfer learning baselines. Across these comparisons, model projection is consistently competitive, particularly when used as an initialization for subsequent fine-tuning, supporting our theoretical perspective that projection allows convolutional networks to inherit favorable optimization properties of feedforward models while substantially reducing the number of trained parameters.

**Contributions.** Our main contributions are:

- We introduce unified, tensor-compatible formalizations of FFN and CNN nodes, enabling precise comparison between the corresponding model classes. Using this framework, we prove an inclusion relationship establishing a rigorous direction of inheritance between the generalized FFN and CNN families.
- We propose *model projection*, a principled construction that freezes per-input transformations and introduces one trainable scalar per input-channel contribution. We prove that projected nodes take the generalized FFN

form, and therefore projected CNNs can inherit FFN results and techniques that do not rely on homogeneous inputs.

- We provide an open-source implementation of projection and demonstrate its practical value for transfer learning across multiple public datasets, showing that projection can adapt entire models while training substantially fewer parameters.

## 1.1. Related Work

**Formalizations and inheritance across model families.** Formal treatments of neural network computations are often specialized to particular architectures and input shapes rather than expressed in a unified, tensor-level language. Classical discussions of feedforward networks typically assume vector-valued (scalar) inputs (Hastie et al., 2009), while standard formulations of convolutional networks are usually presented for specific spatial cases, most commonly 2-dimensional (2D) inputs (LeCun et al., 2010). This separation makes it harder to state precise relationships between the two classes of models, and therefore to rigorously justify when results or techniques from one class should apply to the other. Despite the practical cross-use of ideas between FFNs and CNNs, explicit formal discussions of inheritance between these classes appear limited, motivating general frameworks that clarify which properties are preserved across model classes.

**Parameter-efficient transfer learning (PEFT).** Transfer learning adapts a pretrained model to a downstream task, often in low-data regimes where full fine-tuning can overfit or be difficult to optimize (Chollet, 2021; Han et al., 2024; Jia et al., 2022; Wang et al., 2023). Parameter-efficient approaches mitigate these issues by restricting the set of trainable parameters (Kornblith et al., 2019). Common baselines include updating normalization parameters such as Batch-Norm affine terms (Ioffe & Szegedy, 2015), tuning only bias parameters (Zaken et al., 2022), and feature-modulation schemes that learn lightweight scale and shift parameters (Lian et al., 2022). A complementary line of work introduces small trainable modules, such as residual adapters and their vision-specific variants for ConvNets, to enable adaptation with limited additional parameters (Rebuffi et al., 2017; Chen et al., 2024; Luo et al., 2023). Another widely used direction is low-rank adaptation, where rank-constrained updates are learned while the pretrained backbone is largely frozen (Hu et al., 2022), including variants tailored to convolutional architectures (Ding et al., 2024); related work also studies how to allocate limited tuning capacity across layers based on sensitivity (He et al., 2023). These methods achieve parameter efficiency through parameter subsetting, feature modulation, auxiliary modules, or low-rank reparameterizations; in contrast, model projection freezes pretrained

spatial filters and learns a single scalar value for each contribution, enabling channel-wise reweighting throughout convolutional layers with minimal additional parameters. This differs from pre-defined CNNs, where a set of fixed filters produce outputs that are then sent to a layer of  $1 \times 1$  convolutional nodes (Linse et al., 2023), which we discuss in Remark 3.13.

## 2. Background and Problem

### 2.1. Problem

Our goal is to answer the following questions: *Under what conditions, if any, do CNNs naturally inherit results from FFNs, and vice versa, and, does this inheritance aid in transfer learning?* For example, traditional feed forward neural networks train with fewer parameters per node. When fine tuning a CNN foundation model for a downstream task, can we inherit this property to efficiently train an entire neural network with fewer parameters?

Before introducing the relevant background, we first formalize what is meant by a neural network model. We define a network model  $M := M(\theta)$ , where  $\theta \in \mathbb{R}^p$ , to be some function composed of  $L \in \mathbb{N}$  sequential layers. That is,  $M$  can be expressed as a composition of  $L$  subfunctions or *layers*  $M(\theta) = f_L \circ \dots \circ f_1$ . Given input  $Z_i$  and parameters  $W_i$ , each layer  $f_i$  produces a sequence of at least two outputs  $a_{ij}$ ,  $j = 1, \dots, J_i$ ,  $J_i \geq 2$ . Each output  $a_{ij}$  corresponds to a node  $f_{ij}$  and subset of parameters  $W_{ij}$ . We may refer to  $a_{ij}$  as the  $j$ th *channel* of layer  $i$ . Precisely, each layer can be written as

$$\begin{aligned} f_i(Z_i, W_i) &= [f_{i1}(Z_i, W_{i1}), \dots, f_{iJ_i}(Z_i, W_{iJ_i})] \\ &= [a_{i1}, \dots, a_{iJ_i}] \\ &= [Z_{(i+1,1)}, \dots, Z_{(i+1,J_i)}] = Z_{i+1}. \end{aligned}$$

### 2.2. Traditional Neural Networks

Traditional neural networks (FFNs) are a type of network model, where data flows along edges, and calculations are done in nodes. We summarize the description from Hastie et al. (Hastie et al., 2009). Traditionally, these calculations are linear regressions, followed by a non-linear function  $\sigma$ . Let  $w_j$  be the set of  $W_j$  without bias parameters. Given an input  $Z \in \mathbb{R}^d$ , a parameter set containing a vector of weights  $w_j \in \mathbb{R}^d$ , and a bias  $b_j \in \mathbb{R}$ , the node will have the following form:

$$f_j(Z, W_j) = \sigma\left(\sum_{k=1}^d Z_k W_{jk} + b_j\right). \quad (1)$$

This formulation requires that the input and output data are vectors of scalars. While more general versions have been implemented in code (Chollet, 2021), to the best of

our knowledge, all formal treatments have so far required non-scalar data to be vectorized first.

### 2.3. Convolutional Neural Networks

Convolutional neural networks (CNNs) are another type of network model, but where some nodes perform a convolution. For simplicity, we describe the 2-dimensional case from LeCun et al. (2010), from which the more general case extends naturally. Given an input  $Z \in \mathbb{R}^{d \times n_1 \times n_2}$ , and a parameter set containing a filter  $F_j \in \mathbb{R}^{d \times l_1 \times l_2}$  with filter channels  $F_{jk} \in \mathbb{R}^{l_1 \times l_2}$ , and a bias  $B_j \in \mathbb{R}^{m_1 \times m_2}$ , a convolutional node  $f_j$  will have the following form, where  $*$  denotes the convolution operation:

$$f_j(Z, W_j) = \sigma\left(\sum_k F_{jk} * Z_k + B_j\right). \quad (2)$$

$F_{jk}$  connects input channel  $Z_k$  to output  $a_j$ . We consider the node  $F_j$  to be the collection of operations and parameters connecting  $Z$  to output  $a_j$ , plus the bias. While CNNs often operate on 1-, 2-, or even 3-dimensional data, the common formulations often only specify the 2-dimensional case. For further reading see (LeCun et al., 2010; Chollet, 2021; Goodfellow et al., 2016).

## 3. Inheritance between CNNs and FFNs

### 3.1. Node Generalization and Model Subclasses

We can now address our earlier question of inheritance through *model subclasses* and *model projections*. We start by generalizing equations for commonly used neural network models. In order to do so, we define a generalization of the dot product that outputs a tensor called the tensor dot product. Let a tensor be a multidimensional array with shape  $D$ . Let  $\Gamma_D$  be a tensor of shape  $D$  where all values are 1.

**Definition 3.1.** For  $Z \in \mathbb{R}^{d \times D}$ , and  $w \in \mathbb{R}^d$  the simplified tensor dot product, denoted  $\odot_t$ , is  $Z \odot_t w = \sum_{k=1}^d Z_k w_k$ .

The simplified tensor dot product takes in a vector  $Z$ , of  $d$  tensors,  $Z_k \in \mathbb{R}^D$ , of uniform size and shape  $D$ , as well as a vector of  $d$  scalars,  $w$ , and outputs a tensor of size and shape  $D$ . Here,  $Z_k w_k$  is scalar multiplication. When the size of  $Z_k$  is 1 in all dimensions,  $\odot_t$  reduces to the traditional dot product.

*Remark 3.2.* For ease of exposition, we introduced a simpler version of the tensor dot product, namely  $w$  is assumed to be a vector of scalars, whereas commonly used implementations use a more general tensor dot product for such nodes, such as in dense layers in Tensorflow (Abadi et al., 2015; Chollet, 2021), and linear layers in Pytorch (Ansel et al., 2024).

We now generalize FFN nodes to apply to structures of data

other than vectors of scalars, and define a general convolutional node for a tensor of shape  $D$ . Let  $\Gamma_D$  be a tensor of shape  $D$  where all values are equal to one.

**Definition 3.3.** For  $Z \in \mathbb{R}^{d \times D_{in}}$ ,  $b_j \in \mathbb{R}$ ,  $\Gamma_{D_{out}} \in \mathbb{R}^{D_{out}}$ , and  $W_j \in \mathbb{R}^d$  the GFFN node is:

$$\begin{aligned} f_j(Z, W_j) &= \sigma(Z \odot_t w_j + b_j \Gamma_{D_{out}}). \\ &= \sigma\left(\sum_{k=1}^d Z_k W_{jk} + b_j \Gamma_{D_{out}}\right). \end{aligned} \quad (3)$$

To generalize a FFN node from Equation 1, we can replace  $z \in \mathbb{R}^d$  with  $Z \in \mathbb{R}^{d \times D_{in}}$  and replace  $b_j \in \mathbb{R}$  with  $b_j \Gamma_{D_{out}} \in \mathbb{R}^{D_{out}}$ . In other words,  $Z$  is now a vector of tensors instead of a vector of scalars, and the bias is now a tensor with all values being  $b_j$ . Traditional neural network nodes are a special case of GFFN nodes where the input data is a vector of scalars. If the 3-dimensional input is a sequence of 2D image channels, then a GFFN node acts as a  $1 \times 1$  convolutional node. To act as a fully connected layer in the traditional sense, the input can be flattened first. We now define GCNN nodes.

**Definition 3.4.** For  $F_j \in \mathbb{R}^{d \times D_{F_j}}$ ,  $Z \in \mathbb{R}^{d \times D_{in}}$ , and  $b_j \Gamma_{D_{out}} \in \mathbb{R}^{D_{out}}$  the GCNN node is:

$$\begin{aligned} f_j(Z, W_j) &= \sigma(Z * F_j + b_j \Gamma_{D_{out}}). \\ &= \sigma\left(\sum_{k=1}^d Z_k * F_{jk} + b_j \Gamma_{D_{out}}\right). \end{aligned} \quad (4)$$

That is, to generalize a CNN node from Equation 2, we replace  $F_j \in \mathbb{R}^{d \times l_1 \times l_2}$  with  $F_j \in \mathbb{R}^{d \times D_{F_j}}$ , we replace  $Z \in \mathbb{R}^{d \times n_1 \times n_2}$  with  $Z \in \mathbb{R}^{d \times D_{in}}$ , and we replace  $B_j \in \mathbb{R}^{m_1 \times m_2}$  with  $b_j \Gamma_{D_{out}} \in \mathbb{R}^{D_{out}}$ . Colloquially, the filters and data have the same number of dimensions in each channel, but the number of dimensions is not specified globally for the network. Instead of a vector of 2D images, we now have a vector of tensors. The bias is now a tensor with all values being  $b_j$ .

Now that we have formalized general definitions, we can now prove that the class of traditional feed forward neural network models (FFNs) is a subclass of the class of convolutional neural networks (CNNs).

**Theorem 3.5.** GFFNs are a strict subset of GCNNs.

The proof of this result can be found in Appendix A. To prove Theorem 3.5, we establish a bijection between the set of GFFNs and a subset of GCNNs, namely the set of GCNNs with kernels of size one in all dimensions. An important consequence of Theorem 3.5 is the following.

**Corollary 3.6.** Since the class of GFFNs is contained in the class of GCNNs, any property that holds for all GCNNs also holds for the corresponding subclass of GFFNs.

Corollary 3.6 says that any results or techniques that apply to all GCNNs automatically apply to all GFFNs. Thus, any techniques and results from GCNNs carry over to GFFNs.

### 3.2. Model Projection

Of course, CNNs are not a subclass of FNNs. As a consequence, we now introduce *model projection*: a method to project CNNs and other non-FFN nodes, onto FFN nodes. This allows inheritance of many properties exclusive to FFNs, such as training a node with one weight per input. We first define a node function.

**Definition 3.7.** The *node function*  $f'_j$  associated with a node  $f_j$  is defined by

$$f_j(Z, W_j) = \sigma(f'_j(Z, W_j)),$$

that is,  $f'_j$  is the pre-activation (inner) function of the node.

We now define *separable by input*, a property a node's sub-functions are required to have in order for the node to be projected.

**Definition 3.8.** A node function  $f'_j$  is separable by input if, for an input  $Z$  with  $d$  elements,  $f'_j$  takes the following form:  $f'_j(Z, W_j) = \sum_{k=1}^d f'_{jk}(Z_k, W_{jk}) + b_j \Gamma_{D_{out}}$ , where each  $f'_{jk}$  depends only on the  $k$ th input component  $Z_k$  and a corresponding subset  $W_{jk} \subset W_j$  of parameters.

“Separable by input” means that the node subfunction decomposes into a sum of node sub-functions  $f'_{jk}$  plus a bias, where each  $f'_{jk}$  depends on only one input channel. For example, the function  $g_1(x_1, x_2) = a_1 x_1^2 + a_2 x_2^2 + a_3 x_1 + a_4 x_2$ , where  $a_1, \dots, a_4 \in \mathbb{R}$  is separable by input, since we can write

$$\begin{aligned} g_1(x_1, x_2) &= (a_1 x_1^2 + a_3 x_1) + (a_2 x_2^2 + a_4 x_2) \\ &= g_{11}(x_1) + g_{12}(x_2). \end{aligned}$$

On the other hand, the function  $g_2(x_1, x_2) = a_1 x_1^2 + a_2 x_2^2 + a_3 x_1 + a_4 x_2 + x_1 x_2$  is not separable by input, because of the  $x_1 x_2$  term. GCNN node functions are separable by input, see Lemma A.1 in the Appendix. Node functions that are separable by input can be “projected.”

**Definition 3.9.** Given a node function that is separable by input, its *projected node* is defined as  $\hat{f}_j(Z, W_j, \gamma_j) = \sigma\left(\sum_{k=1}^d \gamma_{jk} f'_{jk}(Z_k, W_{jk}) + b_j \Gamma_{D_{out}}\right)$ . A model's *GFFN projection* is the model that results from projecting all non-GFFN nodes that are separable by input and leaving the rest of the network unchanged.

Here, the idea is that if we view the weights  $W_{jk}$  as fixed, and consider training the new weights  $\gamma_{jk}$  for a downstream task, then the projected model is essentially a GFFN with node-specific pre-processing and inherits all properties, including training techniques, for a GFFN that do not rely on homogeneous inputs, which are discussed next.

We now introduce a property of a layer called *homogeneous inputs*.

**Definition 3.10.** A layer has *homogeneous inputs* if all nodes in the layer have the same input, otherwise it has inhomogeneous inputs. A node has homogeneous inputs if it is part of a layer with homogeneous inputs, otherwise it has inhomogeneous inputs.

Our next result says that projected nodes are GFFN nodes with inhomogeneous inputs.

**Theorem 3.11.** *Projected nodes are GFFN nodes with inhomogeneous inputs.*

*Proof.* Let  $\hat{Z}_{jk}$  denote the output of the node sub-function with fixed weights  $f'_{jk}(Z_k, W_{jk})$ . Then we can rewrite the equation for a projected node as:

$$\begin{aligned}\hat{f}_j(Z, W_j, \gamma_j) &= \sigma\left(\sum_{k=1}^d \gamma_{jk} f'_{jk}(Z_k, W_{jk}) + b_j \Gamma_{D_{out}}\right) \\ &= \sigma\left(\sum_{k=1}^d \gamma_{jk} \hat{Z}_{jk} + b_j \Gamma_{D_{out}}\right) \\ &= \sigma(\hat{Z}_j \odot_t \gamma_j + b_j \Gamma_{D_{out}}).\end{aligned}$$

The final expression above is in the form of Equation 3, with  $Z_j$  replaced by  $\hat{Z}_j$ , and  $W_j$  replaced by  $\gamma_j$ .  $\square$

A direct consequence of Theorem 3.11 is the following.

**Corollary 3.12.** *Since projected nodes are GFFN nodes with inhomogeneous inputs, properties that apply to GFFN nodes with inhomogeneous inputs also apply to projected nodes.*

Corollary 3.12 says that projected layers inherit properties that apply to GFFN layers with inhomogeneous. In particular, given that GCNN node functions are separable by input, see Lemma A.1 in the Appendix, we can project GCNN layers. This is especially useful for transfer learning. For example, GFFN nodes can be trained with one weight per input channel. This is true even in layers with inhomogeneous inputs. Therefore, a projected GCNN node can be trained with one weight per input channel, potentially greatly reducing the total number of parameters being trained.

*Remark 3.13.* A projected CNN differs from a pre-defined CNN (Linse et al., 2023), where a set of fixed filters produce outputs that are then sent to a layer of  $1 \times 1$  convolutional nodes. Instead, each projected node receives a unique input from a single fixed set of filter channels that have not aggregated their channels.

In order to test the usefulness of model projection for transfer learning, we implemented model projection for 2D convolutional layers as a modified version of a 2D convolutional

layer. The main difference is that it also includes a new set of parameters,  $\gamma_{jk}$ , one for each channel,  $k$ , in each convolutional node,  $j$ . We also fix the filter weights, while the new parameters and biases are trained. Each  $\gamma_{jk}$  is initialized to one, so that the first forward pass through the network will be the same as before model projection. Projected nodes learn a linear regression before  $\sigma$  is applied, but unlike a GFFN node, projected nodes also perform an extra pre-processing step to their input. See Algorithm 1 for a step-by-step walk-through of model projection. As stated earlier, an advantage of projecting nodes is that it allows a node to be trained with fewer parameters, reducing the amount of data needed. We explore this idea in the Section 4.

---

#### Algorithm 1 Projection for a node

---

```

1: if node has weights  $W_j$  then
2:   fix all weights except bias
3:   for each channel subfunction,  $f_{jk}$ , in the node do
4:     assign a new multiplicative weight,  $\gamma_{jk}$ , initialized
       to 1
5:   end for
6: end if

```

---

## 4. Experiments

We now demonstrate the utility of inheritance via projection for transfer learning, namely training nodes with only one parameter per input channel. We focus on transfer learning large pre-trained foundation CNN models onto downstream tasks. Normally, CNN nodes can have many parameters per input channel. By projecting these models, we can train an entire model using many fewer parameters, which should be advantageous in cases where there is not data to fully train these large networks.

We conduct two sets of experiments. The first compares model projection with full fine-tuning and logistic regression training, with an emphasis on analyzing training behavior. The second evaluates model projection on standard benchmarks and compares its performance to state-of-the-art parameter-efficient transfer learning methods. We ran our experiments in Google Colab, and our code is available in the supplemental materials.

### 4.1. First Experiment: Understanding Model Projection Behavior

We conduct transfer learning experiments on 7 benchmark datasets, ranging in size from about 2,000 training examples to about 75,000. See Table 1. Our focus is on showing a proof of concept of an example of our method, not on pushing state of the art results, so we intentionally use simple training setups without hyperparameter optimization.

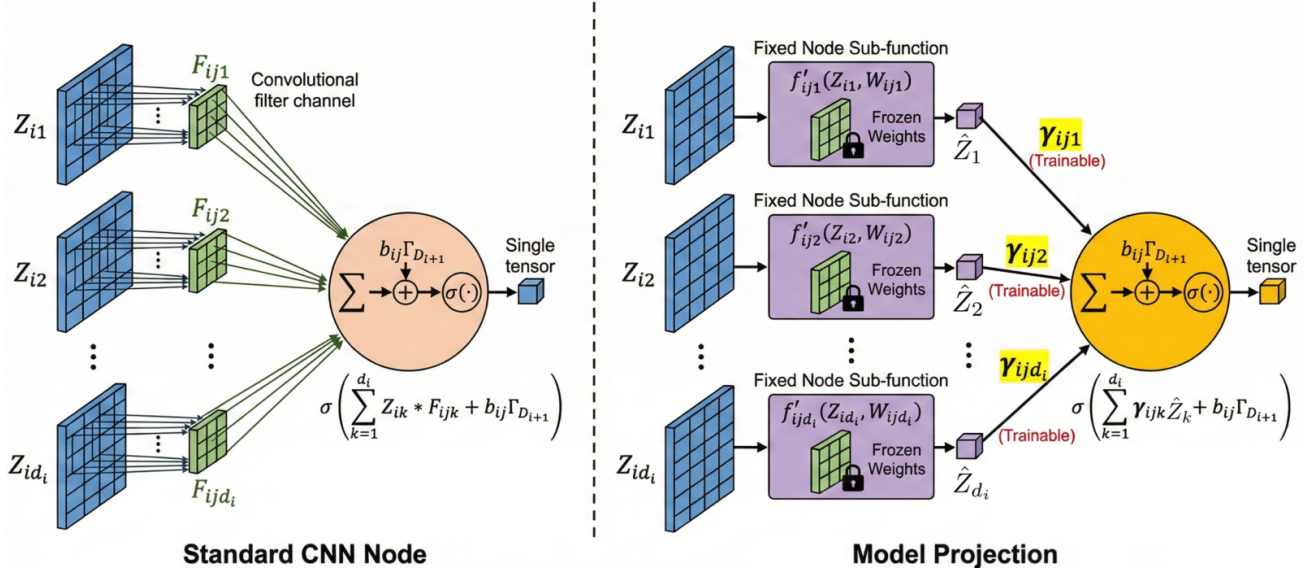


Figure 1. (left) Standard CNN Node: Each input channel contributes through multiple learned weights due to the spatial extent of the kernels. (right) Model projection: The node has exactly one trainable weight per input channel. Spatial structure is preserved by fixed sub-functions, while channel interaction is reduced to a linear weighted sum. The resulting computation is structurally identical to an FFN node with processed tensors as inputs.

Table 1. Benchmark datasets.

Dataset	Classes	Train	Test
Food 101	101	75750	25250
CIFAR 10	10	50000	10000
CIFAR 100	100	50000	10000
Stanford dogs	120	12000	8580
Oxford IIIT pets	37	3680	3669
Caltech 101	102	3060	6084
Oxford 102 flowers	102	2040	6149

**General setup.** We perform experiments using three different convolutional bases, with weights pre-trained on ImageNet(Deng et al., 2009): VGG16(Simonyan & Zisserman, 2015), ResNet50(He et al., 2016), and DenseNet121(Huang et al., 2017). After each convolutional base, we add a global average pooling layer, a dropout layer set to 0.5, and finally a single dense layer for predictions. We use simple data augmentations: horizontal flip with probability 0.5, and random rotation and zoom both set to 0.1. Input images were set to 224 x 224 pixels. We do not shuffle data or address class imbalances. Nor do we address noisy labels or perform any other type of regularization. Any validation sets are absorbed into training sets. We evaluate two training setups:

**Single-stage training.** For each model, we run three variants: Logistic regression (LR), where the backbone is frozen and only the final classifier is trained; Full fine-tuning (FT), where all parameters are trained; and model projection, where convolutional kernels are frozen and all other param-

eters, including projection parameters, are trained. All runs use Adam (Kingma, 2015) with default hyperparameters for 20 epochs.

**Two-stage training.** This setup uses the same models but trains in two stages. Stage 1 runs for 7 epochs with Adam using default hyperparameters. Stage 2 runs for 13 epochs with SGD, learning rate  $10^{-4}$ , momentum 0.9, following the Keras Applications fine-tuning example (Chollet et al., 2015). Under this setup, we evaluate three combinations: Logistic regression in Stage 1, then full fine-tuning in Stage 2 (LR+FT); model projection in Stage 1, then full fine-tuning in Stage 2 (Model projection + FT); and model projection in both stages (2 step model Projection).

We perform the second setup because we observed full fine-tuning occasionally failed to learn in single-stage training, particularly for VGG16. Two-stage training provides a stronger full fine-tuning baseline and allows us to study projection as an alternative warm start to logistic regression training and/or an initialization before full fine-tuning.

## Results.

Results are summarized in Figure 2. Overall, model projection consistently outperforms logistic regression and full fine-tuning across both large and small datasets, and remains robust under older architectures and a simple training setup, while still performing well on newer models. Logistic regression training typically achieves higher initial accuracy but shows limited improvement over epochs, indicating underfitting. Its performance is competitive on smaller datasets

but degrades on larger ones, and it remains relatively robust on older models. Full fine-tuning starts from lower accuracy and improves over training, sometimes surpassing logistic regression training but often struggling on smaller datasets or failing to learn for older architectures such as VGG16. In contrast, model projection combines favorable properties of both approaches: it starts from relatively high accuracy and continues to improve throughout training, achieving the strongest overall performance across experiments.

These results align with what we expect from projection inheritance: strong results from learning an entire neural network, allowing frequent outperformance of logistic regression and greater robustness to dataset size compared to full fine tuning due to inheriting fewer trainable parameters. Model projection retains the expressiveness of end-to-end learning while improving robustness to dataset size and optimization instability. While we expect full fine-tuning to outperform model projection given sufficiently large datasets, and logistic regression training to dominate in extremely low-data regimes (Kornblith et al., 2019), our results suggest that model projection performs best across a broad intermediate regime that covers most practical transfer learning scenarios.

In the two-stage setting, the first stage behaves similarly to the corresponding single-stage experiments, as expected. Notably, performance in the second stage is consistently higher when model projection is used in the first stage, regardless of whether the second stage applies model projection or full fine-tuning. This suggests that model projection provides a more effective initialization for subsequent fine-tuning. Overall, model projection yields stronger performance trends across epochs and emerges as the most effective strategy in the majority of cases. Further details and full results can be found in Appendix B.

#### 4.2. Second Experiment: Model projection Against PEFT Baselines

To evaluate model projection against established parameter-efficient transfer learning (PEFT) approaches, we compare to standard transfer baselines and recent PEFT methods on CIFAR-10, CIFAR-100, and Oxford Flowers on pretrained ResNet50 architecture. Our baselines include logistic regression (training only the final classifier) and full fine-tuning, as well as partial-tuning baselines that update only Batch-Norm parameters (BN) (Ioffe & Szegedy, 2015) along with the final layer, or only bias terms (inspired by BitFit) (Zaken et al., 2022) along with BN and the final layer. This gives a set of methods with gradually increasing trainable parameters on the same model. We additionally compare to low-rank adaptation methods LoRA-r8 and LoRA-r32 (Hu et al., 2022), the Parallel Residual Adapter (PaRA) family (Rebuffi et al., 2017), and the convolutional variant LoRA-C

(Ding et al., 2024). For LoRA-C we report results from Ding et al. (2024), and for LoRA-r8/LoRA-r32 and PaRA we use the ResNet50 results reported by Hedegaard et al. (2024). We include all two-stage variants considered previously.

#### Results

Table 2 summarizes the results. Both single-stage and two-stage model projection are highly competitive across all datasets when compared to PEFT baselines. In particular, the two-stage setup that uses model projection in the first stage, either with full fine tuning or model projection in the second stage, achieves the best performance on CIFAR-10 and CIFAR-100, and the second-best performance on Flowers. These results support the view that model projection provides an effective initialization, especially for subsequent full fine-tuning, by guiding optimization toward more favorable regions of the loss landscape.

Table 2. Performance of our method on the CIFAR 10, CIFAR 100, and flowers datasets, compared to results from other recent methods, all using ResNet50. Values taken from other papers (LoRA-C (Ding et al., 2024) and Para, LoRA-r8, LoRA-r32 (Hedegaard et al., 2024)) are marked with \*.

Method	C10	C100	Flowers
<b>LR</b>	88.20	69.89	87.28
<b>Batch Normalization</b>	95.56	81.22	87.48
<b>BitFit</b>	95.35	81.09	<b>88.50</b>
<b>FT</b>	90.74	73.00	52.81
<b>LR + FT</b>	96.11	82.57	82.94
<b>Model projection</b>	95.99	82.36	87.58
<b>Model projection + F.T.</b>	<b>96.95</b>	<b>84.58</b>	87.51
<b>2-step model projection</b>	96.21	83.57	87.45
<b>LoRA-C</b>	96.59*	82.98*	N/A*
<b>LoRA-r32</b>	95.32*	79.47*	78.57*
<b>LoRA-r8</b>	95.35*	79.22*	80.96*
<b>PaRA</b>	93.52*	79.31*	80.65*

#### 5. Conclusions

In this paper we formalized a general version of the operations of nodes from traditional neural networks and convolutional neural networks. We used this formalization to prove that ffns can inherit from CNNs, but that CNNs cannot inherit from ffns. We proposed *model projection*, a method to project a CNN node onto a ffn node, and proved that this method allows a CNN node to inherit any results or techniques from ffn nodes that do not require homogeneous inputs.

We then demonstrated a proof of concept of our proposed projection method in a transfer learning example. Our method had strong results in a simple setting, reinforcing our theoretical findings. Our example is a good application of projection that we expect will be useful for simple

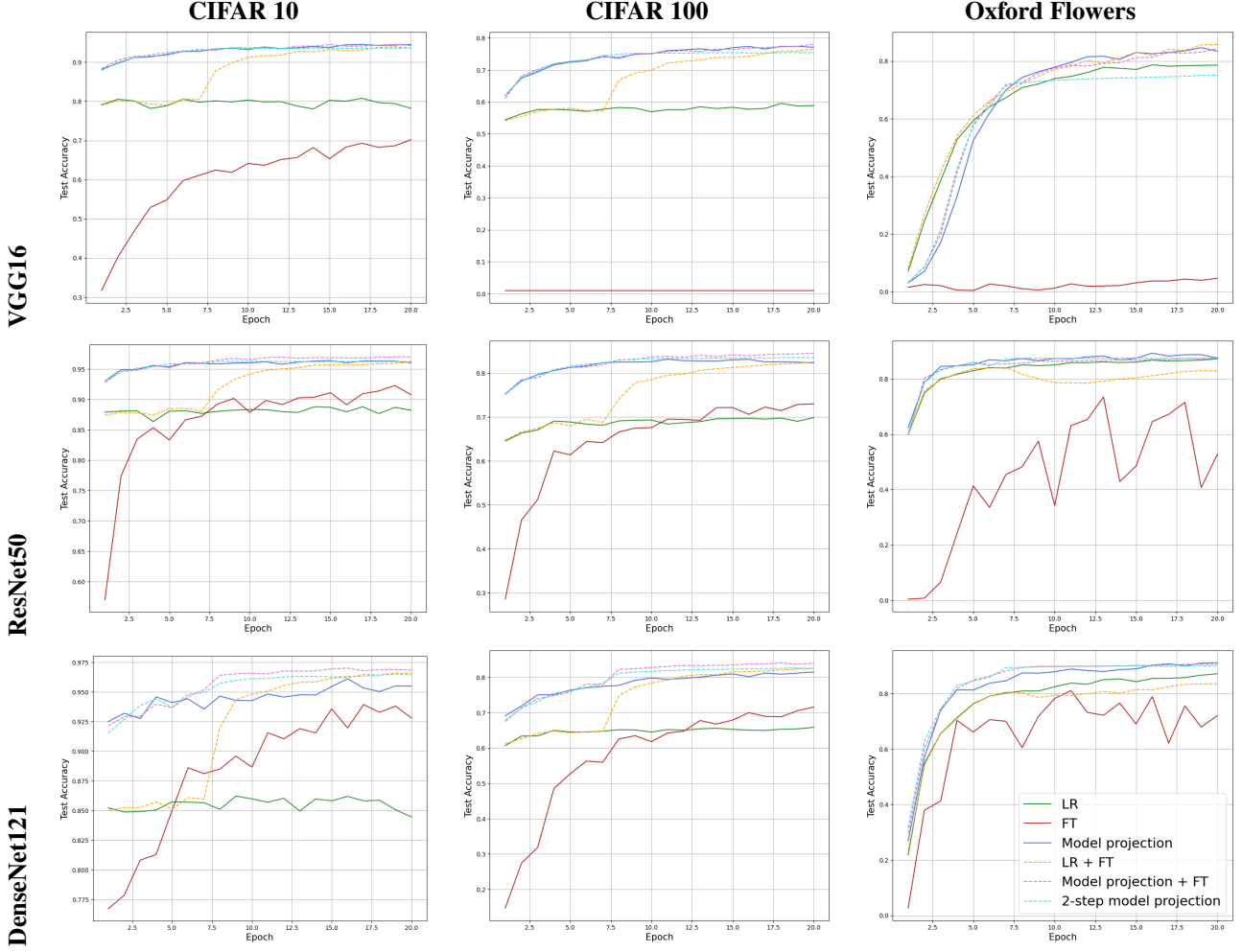


Figure 2. Select results from the first experiments. The solid lines show the single stage setup, while the dashed lines show the two stage setup. Each row corresponds to a particular convolutional base, organized from oldest to most recent. The columns show the results on CIFAR 10, CIFAR 100, and Oxford flowers respectively. In all charts, the x-axis is epochs, and the y-axis is test accuracy.

home made models, and may also be useful in more heavily engineered settings as well.

There are a number of potential directions for future research. Extending analysis of inheritance between more model types such as graph neural networks and transformer models is particularly interesting. More results from ffns can be inherited to CNNs, and exploration of some of these methods such as lasso artificial neural networks (Ma et al., 2022) would be interesting to experiment with. Additionally, further exploration of our example experiment could be done in less simple settings.

## Acknowledgements

The authors acknowledge the support of the Natural Sciences and Engineering Research Council of Canada (NSERC). Cette recherche a été financée par le Conseil

de recherches en sciences naturelles et en génie du Canada (CRSNG), [DGECR-2023-00311, DGECR-2022-04531].

## Impact Statement

“This paper presents work whose goal is to advance the field of Machine Learning. There are many potential societal consequences of our work, none which we feel must be specifically highlighted here.”

## References

Abadi, M., Agarwal, A., Barham, P., Brevdo, E., Chen, Z., Citro, C., Corrado, G. S., Davis, A., Dean, J., Devin, M., Ghemawat, S., Goodfellow, I., Harp, A., Irving, G., Isard, M., Jia, Y., Jozefowicz, R., Kaiser, L., Kudlur, M., Levenberg, J., Mané, D., Monga, R., Moore, S., Murray, D., Olah, C., Schuster, M., Shlens, J., Steiner, B., Sutskever,

I., Talwar, K., Tucker, P., Vanhoucke, V., Vasudevan, V., Viégas, F., Vinyals, O., Warden, P., Wattenberg, M., Wicke, M., Yu, Y., and Zheng, X. TensorFlow: Large-scale machine learning on heterogeneous systems, 2015. URL <https://www.tensorflow.org/>. Software available from tensorflow.org.

Ansel, J., Yang, E., He, H., Gimelshein, N., Jain, A., Voznesensky, M., Bao, B., Bell, P., Berard, D., Burovski, E., Chauhan, G., Chourdia, A., Constable, W., Desmaison, A., DeVito, Z., Ellison, E., Feng, W., Gong, J., Gschwind, M., Hirsh, B., Huang, S., Kalambarkar, K., Kirsch, L., Lazos, M., Lezcano, M., Liang, Y., Liang, J., Lu, Y., Luk, C., Maher, B., Pan, Y., Puhrsch, C., Reso, M., Saroufim, M., Siraichi, M. Y., Suk, H., Suo, M., Tillet, P., Wang, E., Wang, X., Wen, W., Zhang, S., Zhao, X., Zhou, K., Zou, R., Mathews, A., Chanan, G., Wu, P., and Chintala, S. PyTorch 2: Faster Machine Learning Through Dynamic Python Bytecode Transformation and Graph Compilation. In *29th ACM International Conference on Architectural Support for Programming Languages and Operating Systems, Volume 2 (ASPLOS '24)*. ACM, April 2024. doi: 10.1145/3620665.3640366. URL <https://docs.pytorch.org/assets/pytorch2-2.pdf>.

Bossard, L., Guillaumin, M., and Van Gool, L. Food-101 – mining discriminative components with random forests. In *European Conference on Computer Vision*, 2014.

Chen, H., Tao, R., Zhang, H., Wang, Y., Li, X., Ye, W., Wang, J., Hu, G., and Savvides, M. Conv-adapter: Exploring parameter efficient transfer learning for convnets. In *Proceedings of the IEEE/CVF conference on computer vision and pattern recognition*, pp. 1551–1561, 2024.

Chollet, F. Deep learning with python. 2021.

Chollet, F. et al. Keras. <https://keras.io>, 2015.

Deng, J., Dong, W., Socher, R., Li, L.-J., Li, K., and Fei-Fei, L. Imagenet: A large-scale hierarchical image database. In *2009 IEEE conference on computer vision and pattern recognition*, pp. 248–255. Ieee, 2009.

Ding, C., Cao, X., Xie, J., Fan, L., Wang, S., and Lu, Z. Lora-c: Parameter-efficient fine-tuning of robust cnn for iot devices. *arXiv preprint arXiv:2410.16954*, 2024.

Fei-Fei, L., Fergus, R., and Perona, P. Learning generative visual models from few training examples: An incremental bayesian approach tested on 101 object categories. *Computer Vision and Pattern Recognition Workshop*, 2004.

Goodfellow, I., Bengio, Y., and Courville, A. *Deep learning*. MIT press, 2016.

Han, C., Wang, Q., Cui, Y., Wang, W., Huang, L., Qi, S., and Liu, D. Facing the elephant in the room: Visual prompt tuning or full finetuning? In *The Twelfth International Conference on Learning Representations*, 2024.

Hastie, T., Tibshirani, R., and Friedman, J. H. *The elements of statistical learning: data mining, inference, and prediction*, volume 2. Springer, 2009.

He, H., Cai, J., Zhang, J., Tao, D., and Zhuang, B. Sensitivity-aware visual parameter-efficient fine-tuning. In *Proceedings of the IEEE/CVF International Conference on Computer Vision*, pp. 11825–11835, 2023.

He, K., Zhang, X., Ren, S., and Sun, J. Deep residual learning for image recognition. In *Proceedings of the IEEE conference on computer vision and pattern recognition*, pp. 770–778, 2016.

Hedegaard, L., Alok, A., Jose, J., and Iosifidis, A. Structured pruning adapters. *Pattern Recognition*, 156:110724, 2024. ISSN 0031-3203. doi: <https://doi.org/10.1016/j.patcog.2024.110724>. URL <https://www.sciencedirect.com/science/article/pii/S0031320324004758>.

Hu, E. J., Shen, Y., Wallis, P., Allen-Zhu, Z., Li, Y., Wang, S., Wang, L., Chen, W., et al. Lora: Low-rank adaptation of large language models. *ICLR*, 1(2):3, 2022.

Huang, G., Liu, Z., Van Der Maaten, L., and Weinberger, K. Q. Densely connected convolutional networks. In *Proceedings of the IEEE conference on computer vision and pattern recognition*, pp. 4700–4708, 2017.

Ioffe, S. and Szegedy, C. Batch normalization: Accelerating deep network training by reducing internal covariate shift. In *International conference on machine learning*, pp. 448–456. pmlr, 2015.

Jia, M., Tang, L., Chen, B.-C., Cardie, C., Belongie, S., Hariharan, B., and Lim, S.-N. Visual prompt tuning. In *European conference on computer vision*, pp. 709–727. Springer, 2022.

Khosla, A., Jayadevaprakash, N., Yao, B., and Fei-Fei, L. Novel dataset for fine-grained image categorization. In *First Workshop on Fine-Grained Visual Categorization, IEEE Conference on Computer Vision and Pattern Recognition*, Colorado Springs, CO, June 2011.

Kingma, D. P. Adam: A method for stochastic optimization. In *International Conference on Learning Representations (ICLR 2015)*, 2015.

Kornblith, S., Shlens, J., and Le, Q. V. Do better imagenet models transfer better? In *Proceedings of the IEEE/CVF conference on computer vision and pattern recognition*, pp. 2661–2671, 2019.

Krizhevsky, A. Learning multiple layers of features from tiny images. Technical report, 2009.

LeCun, Y., Kavukcuoglu, K., and Farabet, C. Convolutional networks and applications in vision. In *Proceedings of 2010 IEEE international symposium on circuits and systems*, pp. 253–256. IEEE, 2010.

Lian, D., Zhou, D., Feng, J., and Wang, X. Scaling & shifting your features: A new baseline for efficient model tuning. *Advances in Neural Information Processing Systems*, 35:109–123, 2022.

Linse, C., Barth, E., and Martinetz, T. Convolutional neural networks do work with pre-defined filters. In *2023 International Joint Conference on Neural Networks (IJCNN)*, pp. 1–8. IEEE, 2023.

Luo, G. et al. Repadapter: Parameter-efficient and computationally friendly adapter for giant vision models, 2023.

Ma, X., Sardy, S., Hengartner, N., Bobenko, N., and Lin, Y. T. A phase transition for finding needles in nonlinear haystacks with lasso artificial neural networks. *Statistics and Computing*, 32(6):99, 2022.

Nilsback, M.-E. and Zisserman, A. Automated flower classification over a large number of classes. In *Proceedings of the Indian Conference on Computer Vision, Graphics and Image Processing*, Dec 2008.

Parkhi, O. M., Vedaldi, A., Zisserman, A., and Jawahar, C. V. Cats and dogs. In *IEEE Conference on Computer Vision and Pattern Recognition*, 2012.

Rebuffi, S.-A., Bilen, H., and Vedaldi, A. Learning multiple visual domains with residual adapters. *Advances in neural information processing systems*, 30, 2017.

Simonyan, K. and Zisserman, A. Very deep convolutional networks for large-scale image recognition. In *3rd International Conference on Learning Representations (ICLR 2015)*. Computational and Biological Learning Society, 2015.

Wang, D., Wang, X., Wang, L., Li, M., Da, Q., Liu, X., Gao, X., Shen, J., He, J., Shen, T., et al. A real-world dataset and benchmark for foundation model adaptation in medical image classification. *Scientific Data*, 10(1): 574, 2023.

Zaken, E. B., Goldberg, Y., and Ravfogel, S. Bitfit: Simple parameter-efficient fine-tuning for transformer-based masked language-models. In *Proceedings of the 60th Annual Meeting of the Association for Computational Linguistics (Volume 2: Short Papers)*, pp. 1–9, 2022.

## A. Supplementary proofs

*Proof of Theorem 3.5.* We will prove the theorem by showing a bijection between GFFNs and a subset of GCNNs. Suppose that we have a GCNN node where  $F_{jk}$  has size 1 in all dimensions. This means  $F_{jk}$  is a scalar, and  $F_j$  is a vector of scalars. As a result,  $Z_k * F_{jk} = Z_k F_{jk}$ . Using this fact, and the definition of GCNN nodes, we can write:

$$f_j(Z, W_j) = \sigma(Z * F_j + b_j \Gamma_{D_{out}}) = \sigma\left(\sum_{k=1}^d Z_k * F_{jk} + b_j \Gamma_{D_{out}}\right) = \sigma\left(\sum_{k=1}^d Z_k F_{jk} + b_j \Gamma_{D_{out}}\right).$$

Note that  $\sum_{k=1}^d Z_k F_{jk} = Z \odot_t F_j$  by definition. As a result, we have that

$$\sigma\left(\sum_{k=1}^d Z_k F_{jk} + b_j \Gamma_{D_{out}}\right) = \sigma(Z \odot_t F_j + b_j \Gamma_{D_{out}}).$$

Observe that the right-hand side is exactly the definition of GFFN node. Every GCNN node with  $F_{jk}$  of size 1 in all dimensions maps to exactly one GFFN node. We now show the inverse. Suppose we have a GFFN node, viz.

$$f_j(Z, W_j) = \sigma(Z \odot_t W_j + b_j \Gamma_{D_{out}}) = \sigma\left(\sum_{k=1}^d Z_k W_{jk} + b_j \Gamma_{D_{out}}\right).$$

Note that since  $W_{jk}$  is a scalar,  $\sum_{k=1}^d Z_k W_{jk} = \sum_{k=1}^d Z_k * W_{jk}$ . As a result, we have that

$$\sigma\left(\sum_{k=1}^d Z_k W_{jk} + b_j \Gamma_{D_{out}}\right) = \sigma\left(\sum_{k=1}^d Z_k * W_{jk} + b_j \Gamma_{D_{out}}\right).$$

Observe that the right hand side is exactly the definition of a GCNN node, where the kernels have size 1 in all dimensions. Every GFFN node maps to exactly one GCNN node with kernels of size 1.

Therefore, there is a bijection between the subset of GCNNs with kernel size 1 in all dimensions, and the set of GFFNs. Therefore, GFFNs are a subset of GCNNs.  $\square$

### A.1. Projection

**Lemma A.1.** *GCNN node functions are separable by input.*

*Proof.* From Definition 3.4 we have that GCNN node functions can be written as:

$$\sum_{k=1}^d Z_k * F_{jk} + b_j \Gamma_{D_{out}} = \sum_{k=1}^d f'_{jk}(Z_k, W_{jk}) + b_j \Gamma_{D_{out}}.$$

Here,  $f'_{jk}$  is a convolution, and  $W_{jk}$  are the weights in filter channel  $F_{jk}$ .  $\square$

**Lemma A.2.** *If all node functions are separable by input, and all node sub-functions,  $f'_{jk}$ , are associative for scalar multiplication, then  $\gamma_{jk}$  can be applied either before, or after  $f'_{jk}$  acts on  $Z_k$ .*

*Proof.* Each node is separable by input, therefore, we can just consider each node sub-function. Since all node sub-functions,  $f'_{jk}$ , are associative for scalar multiplication, then  $f'_{jk}(\gamma_{jk} Z_k) = \gamma_{jk} f'_{jk}(Z_k)$ .  $\square$

**Proposition A.3.** *In a GCNN node,  $\gamma_{jk}$  can be applied either before, or after  $f'_{jk}$  acts on  $Z_k$ .*

*Proof.* Convolutions are associative for scalar multiplication, therefore, this follows from Lemmas A.1 and A.2.  $\square$

## B. Supplementary results

We now discuss the results from the first set of single stage experiments, seen in Figure 3, with summarizing information presented in Tables 3, 4, and 5. Figure 3 shows that model projection consistently had strong results, while training was relatively smooth and fast. Table 3 shows the ranking of each method across each experiment. Model projection significantly outperformed both the logistic regression and full fine tuning in this simple setup, producing the best model about 81% of the time, and the second best about 19% of the time.

Table 4 shows the rankings achieved by model projection organized by model. Model projection had consistently strong results on each model. Table 5 shows the rankings for model projection grouped by dataset. Model projection had the best scores on all five datasets that were not exclusively pet related, but did not do as well on the two datasets that were exclusively pet related. Interestingly, model projection did well on datasets both larger and smaller than the pet ones, suggesting the issue is not solely dataset size.

*Table 3.* Ranking of each training method in the 21 experiments from the first experimental setup. In a particular experiment (setup, convolutional base, and dataset combination), the method producing the highest test accuracy at the end of the last epoch was designated '1st', the second highest '2nd', and so on.

Method	1st	2nd	3rd
<b>Model projection</b>	17	4	0
<b>Logistic regression</b>	4	11	6
<b>Full fine tuning</b>	0	6	15

*Table 4.* Ranking of Model projection in the 21 experiments from the first experimental setup, organized by convolutional base. In a particular experiment (setup, convolutional base, and dataset combination), the method producing the highest test accuracy at the end of the last epoch was designated '1st', the second highest '2nd', and so on.

Model	1st	2nd	3rd
<b>VGG16</b>	6	1	0
<b>ResNet50</b>	6	1	0
<b>DenseNet121</b>	5	2	0

*Table 5.* Ranking of Model projection in the 21 experiments from the first experimental setup, organized by dataset. In a particular experiment (setup, convolutional base, and dataset combination), the method producing the highest test accuracy at the end of the last epoch was designated '1st', the second highest '2nd', and so on.

Dataset	1st	2nd	3rd
<b>Food 101</b>	3	0	0
<b>CIFAR 10</b>	3	0	0
<b>CIFAR 100</b>	3	0	0
<b>Stanford dogs</b>	1	2	0
<b>Oxford IIIT pets</b>	1	2	0
<b>Caltech 101</b>	3	0	0
<b>Oxford 102 flowers</b>	3	0	0

**Figure 3.** Results from the first set of experiments. The blue lines show the performance of model projection. The green and red lines show the performances of the single layer logistic regression, and the full fine tuning respectively. Each column corresponds to a particular convolutional base, organized from oldest to most recent. Each row shows the results on a particular dataset, organized from largest to smallest. In all charts, the x-axis is epochs, and the y-axis is test accuracy.

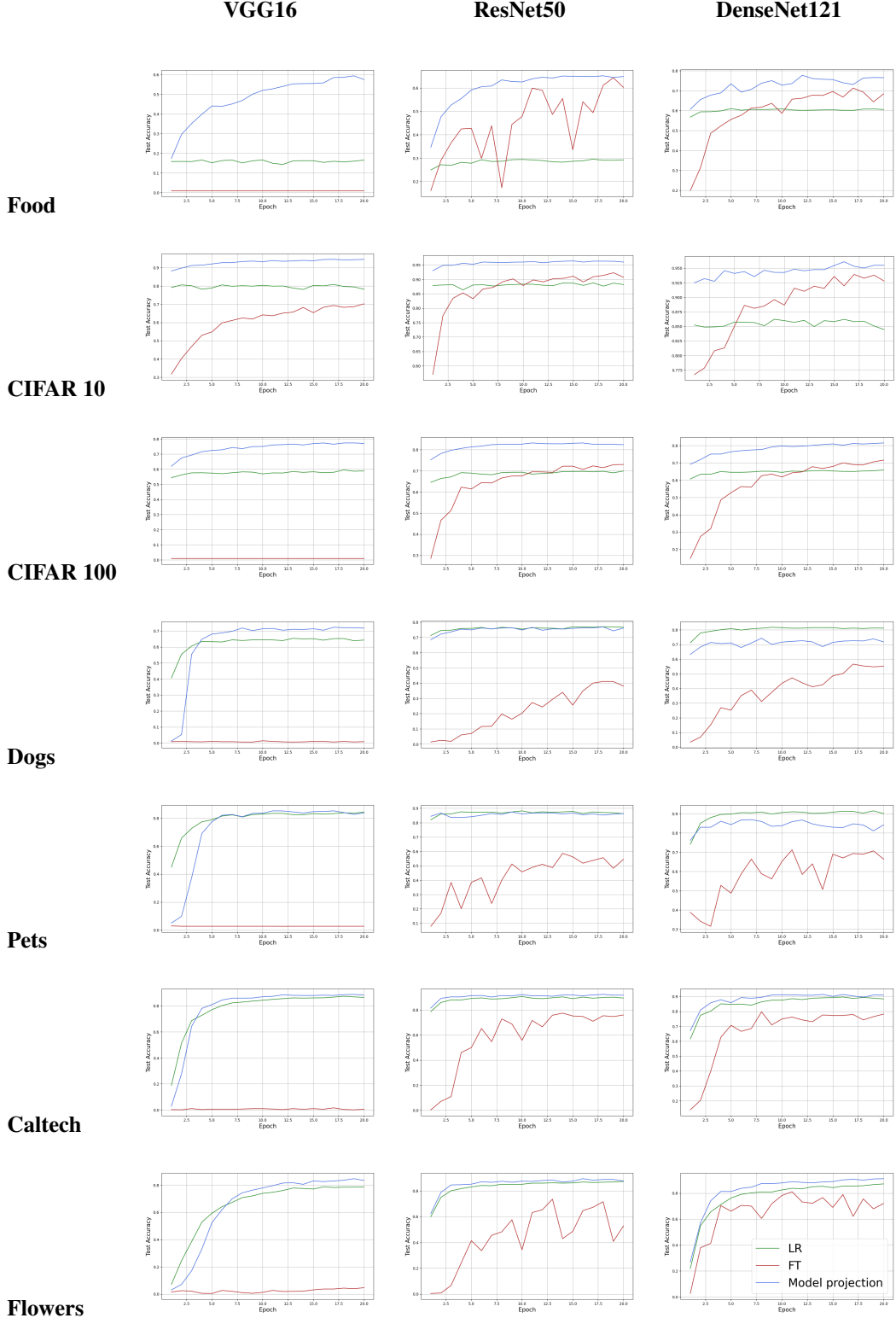


**Figure 4.** Results from the second set of experiments. The orange lines show the performance of 2-step fine tuning. The pink lines show the performance of 2-step fine tuning using projection in the first step, and the light blue lines represent the performance of the 2-steps using projection in both steps. Each column corresponds to a particular convolutional base, organized from oldest to most recent. Each row shows the results on a particular dataset, organized from largest to smallest. In all charts, the x-axis is epochs, and the y-axis is test accuracy.

